Structural characterization of water and ice in mesoporous SBA-15 silicas: II. The 'almost-filled' case for 86 Å pore diameter

2008 J. Phys.: Condens. Matter 20 205107

(http://iopscience.iop.org/0953-8984/20/20/205107)

J. Phys.: Condens. Matter **20** (2008) 205107 (10pp) doi:10.1088/0953-8984/20/20/205107

Structural characterization of water and ice in mesoporous SBA-15 silicas: II. The 'almost-filled' case for 86 Å pore diameter

J Seyed-Yazdi[1,2], H Farman[1], John C Dore[2], J Beau W Webber[2,3,4], G H Findenegg[5] and T Hansen[6]

[1] Iran University of Science and Technology, Narmak, Tehran, Iran
[2] School of Physical Sciences, University of Kent, Canterbury CT2 7NH, UK
[3] Institute of Petroleum Engineering, Heriot Watt, Edinburgh EH14 4AS, UK
[4] Lab-Tools Ltd, G17 Canterbury Enterprise Hub, University of Kent, CT2 7NJ, UK
[5] Department of Chemistry, Technical University Berlin, Strasse des 17 Juni 124, D-10623 Berlin, Germany
[6] Institut Laue Langevin, BP156, F38042 Grenoble Cedex, France

E-mail: J.C.Dore@kent.ac.uk

Received 12 November 2007, in final form 8 April 2008
Published 1 May 2008
Online at stacks.iop.org/JPhysCM/20/205107

Abstract

Neutron diffraction measurements for D_2O in SBA-15 silica of pore diameter 86 Å have been made in a temperature range from 300 to 100 K. The pore-filling factor for the liquid phase is 0.95, resulting in an 'almost-filled' sample. The nucleation and transformation of the ice phase were determined for cooling and warming cycles at two different rates. The primary nucleation event at 258 K leads to a defective form of ice-I with predominantly cubic ice features. For temperatures below the main nucleation event, the data indicate the formation of an interfacial layer of disordered water/ice that varies with temperature and is reversible. The main diffraction peak for the water phase shows similar features to those observed in earlier studies, indicating enhanced hydrogen bonding and network correlations for the confined phase as the temperature is decreased. A detailed profile analysis of the triplet peak is presented in the accompanying paper (Seyed-Yazdi *et al* 2008 *J. Phys.: Condens. Matter* **20** 205108).

(Some figures in this article are in colour only in the electronic version)

1. Introduction

The characteristics of water in a confined geometry are significantly changed from those of the bulk state. Extensive studies have been made for water in a wide range of mesoporous silicas using a range of experimental techniques. A review of neutron and NMR results for water/ice in various forms of silica has been published (Webber and Dore 2004) The basic information shows that the nucleation temperature is depressed and the resultant ice formed in the pores has a defective cubic ice structure rather than the normal form of hexagonal ice. Initial studies were made on sol–gel or leached silica samples but more recent work has focused on the ordered mesoporous silicas, such as MCM and SBA materials, prepared by templating techniques. These materials have a regular cylindrical pore structure of small polydispersity with dimensions covering the range 20–100 Å.

The silica surface has a hydrophilic interaction with the water and the results indicate that there is an interfacial layer of water/ice that has a different behaviour from the rest of the water in the pore. In this context, it has been interesting to study the characteristics for materials of varying pore diameter and also partial filling of the pore volume. The work by Findenegg and colleagues (Schreiber *et al* 2001, Grünberg *et al* 2004) for a series of MCM and SBA silicas demonstrates the complexity that arises in the nucleation process. The detailed structural features of the water and ice phases can be conveniently studied by neutron diffraction and a recent paper (Liu *et al* 2006) has provided information for an over-filled sample of SBA-15 silica with a pore diameter of 86 Å.

Table 1. The temperature sequence for the three separate cycles.

T start (K)	T final (K)	Mode: range	Rate (K min^{-1})	No. of points
300	204	cooling: 96 K	2.0	31
204	300	heating: 96 K	2.0	24
300	250	cooling: 50 K	0.2	49
250	289	heating: 39 K	0.2	58
289	102	cooling: 187 K	0.2	92
102	249	heating: 147 K	0.2	48

The present paper extends this work to the study of an 'almost-filled' sample of the same material and investigates the behaviour of the water/ice components over a temperature range of 100–300 K. A quantitative analysis of the profile for the main diffraction peak consisting of several overlapping components is presented in the accompanying paper (Seyed-Yazdi *et al* 2008), Paper 3.

2. Experimental measurements

As for the previously-reported measurements (Liu *et al* 2006), the experiment was conducted on the D20 diffractometer (Hansen *et al* 2008) at the Institut Laue Langevin, Grenoble, using an incident neutron wavelength of 2.400 ± 0.005 Å. Details of the sample preparation are given in that paper; the current measurements were made during the same experimental run. The sample studied in the present work was prepared from the same SBA-15 material with added D_2O corresponding to filling factor of 0.95 ± 0.03, whereas the previous measurements were made for an over-filled sample with a filling factor of approximately 1.15. Similar studies for filling factors of 0.60 and 0.40 will be reported in a later paper. Measurements were made for the dry silica sample and the 'wet' silica sample, covering a Q-range of 0.3 to 5.1 Å^{-1}, as reported, previously. Measurements were made with a constant temperature ramp in both cooling and heating mode. The temperature ramp was either a 'fast' rate of 2 K min^{-1} or a 'slow' rate of 0.2 K min^{-1}. The diffraction pattern was recorded every 2 min and five datasets were added together to give a suitable statistical accuracy for the analysis procedure. The usual data processing was conducted to convert the recorded data into an intensity pattern as a function of the scattering vector, Q, at various temperature intervals. It was found convenient to make measurements over a wide temperature range as the intensity of the ice peaks was seen to be changing systematically even for temperatures below 200 K. The full set of runs is indicated in table 1.

3. Results

Measurements were made for a temperature range that included both the super-cooled water and the variable ice phases. The ice profile was observed to retain the same basic shape and was similar to that seen in the study of the over-filled case ($f = 1.15$) presented earlier (Liu *et al* 2006) but without the hexagonal ice component formed on the outside of the silica grains. A typical measurement for the wet and dry silica

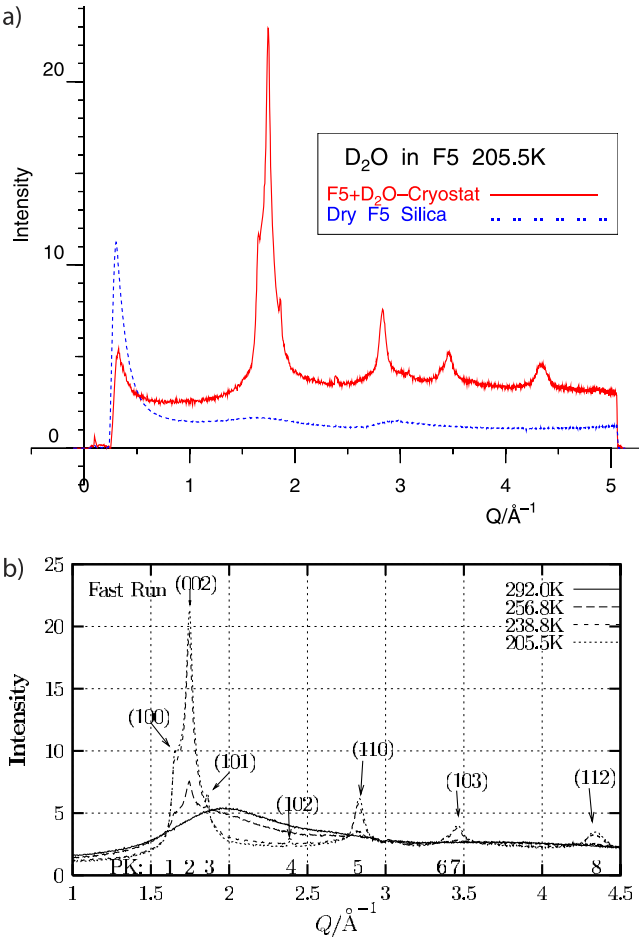

Figure 1. (a) The diffraction pattern for the wet and dry SBA-15 (F5) silica at 205 K. (b) The diffraction pattern for various phases of water/ice in a SBA-15 silica for a pore diameter of 86 Å and filling factor of $f = 0.95$.

is shown in figure 1(a), indicating the relatively low scattering intensity from the substrate. The behaviour in the low-Q region ($Q < 1$ Å^{-1}) is indicative of the change in the tail region of the SANS intensity from the filling of the pore volume, resulting in a decreased contrast for the filled sample. The initial stage of data analysis fitted and removed this Q^{-4} SANS component. As shown in figure 1(b), the first diffraction 'peak' in the region of 1.7 Å^{-1} is broad and incorporates three components (1, 2 and 3) in the profile that relate to the triplet seen for hexagonal ice. However, the overall profile is markedly asymmetric and the peaks overlap each other, indicating the formation of a defective or disordered phase of ice-I. The unique peak (4) at 2.39 Å^{-1} for I_h ice is almost entirely absent although a small residual peak is usually found in this position. The overall scattering level above the triplet peak is higher than that on the low-Q side, indicating the presence of a diffuse scattering component arising from some form of disorder in the water/ice structure. The remaining four peaks (5, 6, 7 and 8) are also broad in comparison with the hexagonal ice peaks observed for the over-filled case (Liu *et al* 2006) but do not display the asymmetry of the composite peak.

The results may be treated either in terms of the total diffraction pattern for the ice/water phase as a function

of temperature or by the use of the temperature-difference function, which emphasizes the variation in the profile with respect to a chosen reference temperature. For the total pattern, the diffraction profile is composed of an intra-molecular term, $f_1(Q)$, and an inter-molecular term, $D_M(Q)$, such that the structure factor is conventionally written for the liquid case as:-

$$S_M(Q) = f_1(Q) + D_M(Q). \quad (1)$$

The same expression applies to the glassy state but it is more conventional to write the expression for the crystalline state in terms of the structure factor $S(hkl)$ to emphasize the ordered lattice structure. However, both expressions arise from coherent interference in the scattered beam and are equivalent, such that the measured intensity, $I(Q)$, after treatment for experimental and analytic corrections, is proportional to the structure factor in each case. In order to emphasize the structural changes and the formation of the ice from the water phase, it is convenient to use the temperature-difference function, $\Delta I(Q, T; T_0)$, defined as:-

$$\Delta I(Q, T; T_0) = I(Q, T) - I(Q, T_0) = \Delta D_M(Q, T; T_0) \quad (2)$$

for the measured intensity, $I(Q, T)$, where T_0 is a reference temperature. This function is useful, as the substrate contribution from the silica and the intra-molecular form-factor, $f_1(Q)$, for the individual water molecules, are automatically removed by the subtraction process. Consequently, the derived function is a direct measurement of structural variation within the ice/water system and is a highly sensitive method of observing subtle changes in the phase stability and transformation of the different components. Both of these methods are appropriate as they illustrate different features in the data. However, the composite nature of the main diffraction peak requires special treatment and a detailed analysis is presented in Paper 3.

4. Analysis

4.1. Variation with ramp rate

The two cooling and warming runs were made at different temperature ramp rates, firstly at 2 K min^{-1} and secondly at 0.2 K min^{-1}. The slower ramp rate provided 250 individual datasets covering a temperature range of 300–102 K and was the main sequence to be analysed due to the higher statistical accuracy of the observations for corresponding temperature intervals. The faster ramp rate yielded 60 datasets over the temperature range, 300–204 K. Several different states were covered in the cooling sequence, including normal water, super-cooled water, nucleation of cubic ice and subsequent growth of defective ice-I over the lower temperature range; these phase changes are reversed on the heating cycle. The main freezing and melting events in the pores occur at different temperatures but the phase changes over the rest of the temperature cycle are surprisingly reversible (Webber *et al* 2008). The diffraction patterns obtained for these different regions are shown superimposed in figure 1(b) for the fast ramp rate, incorporating the summation of five sequential datasets for the cooling ramp. The ice peaks may be characterized by the Miller indices shown on the diagram.

The first three peaks appear to correspond to the triplet of hexagonal ice, whereas pure cubic ice should have only one peak at the centre of the triplet. The fourth Bragg peak at 2.39 Å^{-1} arises only for hexagonal ice and in the current studies is present only as a small contribution, although it does have some significance in the subsequent analysis, as shown below (sections 4.2 and 4.3). The fifth crystalline peak at 2.83 Å^{-1} has a significant intensity and includes contributions from both ice forms. It also appears to sit on top of a much broader 'oscillatory' background that arises from structure features in the diffuse scattering contribution.

It was found that the results for the two ramp rates were very similar but not completely identical. The main difference concerned the small contribution due to the definitive hexagonal ice peak at 2.39 Å^{-1} and the associated peaks in the main triplet, where the weak peak 3 at 1.86 Å^{-1} shows a difference in relative intensity for the two runs. These observations imply that the amount of hexagonal ice is higher in the first run with the faster cooling rate. An examination of the different temperatures revealed that the initial stages of the nucleation did not contain any evidence of hexagonal ice formation, as judged from peaks 3 and 4; the emergence of these two peaks occurred simultaneously at a slightly lower temperature. This feature is shown in figure 2(a) for the sequence of individual datasets corresponding to the nucleation sequence, where the ice peaks increase in magnitude as the broad water peak is reduced. Both the water and the ice are present due to a significant temperature gradient of 2 K across the sample but it is clear that the onset of nucleation occurs at a specific well-defined temperature. Surprisingly, the heating run follows a similar but reversed behaviour, as the hexagonal ice peaks disappear before the main reduction in the magnitude of the cubic ice peak, as shown in figure 2(b) This phenomenon is puzzling and further comment is deferred to section 5.

For the main analysis, the different runs were added together in groups of five to yield datasets with a higher statistical accuracy. The faster rate was also averaged over five runs and therefore covered a larger temperature interval in each of the 11 datasets for a range of 300–204 K.

4.2. Ice structure: peaks 5, 7 and 8

The peaks 5, 7 and 8 were analysed using a peak-fitting routine to determine the position, width and intensity of the peaks. The broad peak 6 cannot be treated in the same way and does not correspond to any known features of ice-I; its presence is presumably related to the defective nature of the ice I_c component. The function defining each sharp peak contains three variable parameters and has the form:-

$$I(Q, i) = \frac{I_0(i)}{\cosh\left[(Q - Q_0(i))/\sigma(i)\right]} \quad (3)$$

where $I_0(i)$ is the magnitude of each peak, $Q_0(i)$ is the peak position, $\sigma(i)$ is a width parameter and i is the index for each of the peaks. This 'sech' form was used in preference

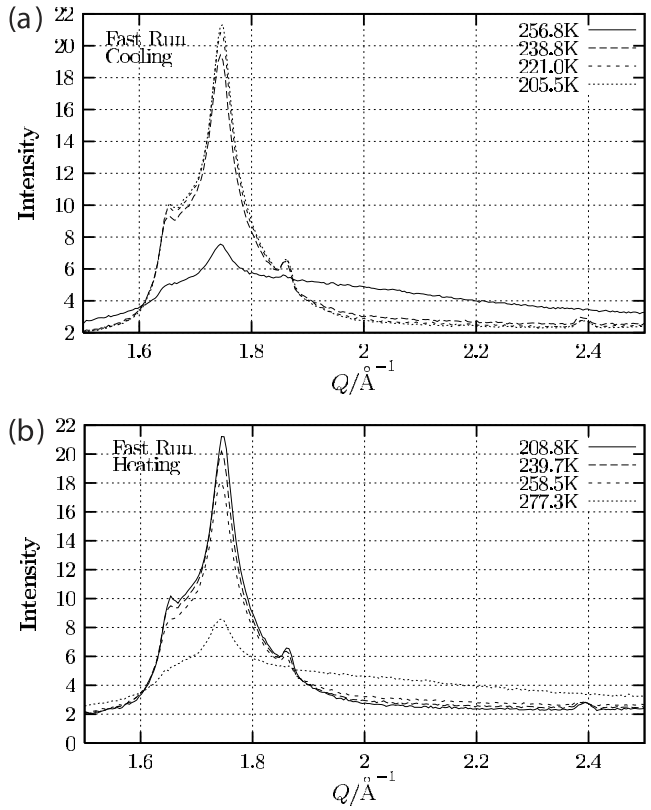

Figure 2. Variation of the diffraction pattern for peaks 1–4 during (a) nucleation and (b) melting.

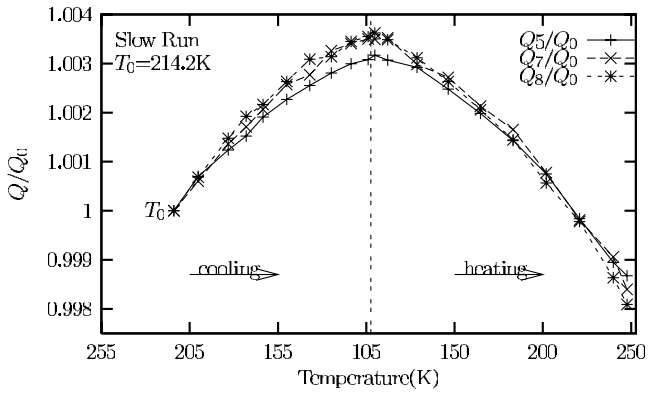

Figure 3. Variation of the peak positions (5, 7, 8) with temperature, $Q_0(T)$, for cooling and heating run.

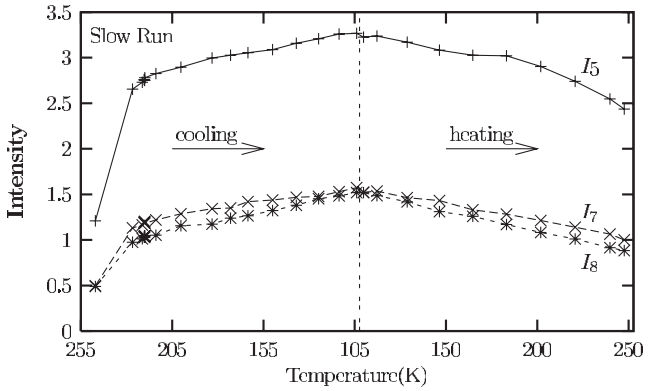

Figure 4. Variation of the peak intensities (5, 7, 8) with temperature, for cooling and heating runs.

to a Gaussian curve as it has slightly broader wings and was thought to be more appropriate for the observed data. The difference in functional form is not expected to contribute significantly to the conclusions drawn from the parameter variation. The fits were carried out using a normal χ^2-minimisation routine (Evans 1997) and were found to vary with temperature in a systematic manner. It was then possible to fix the width parameters at constant values and to optimize the final fit by varying the other parameter values defining the position and intensity. The relative parameter values for the peak positions are shown in the form of a $Q(i)/Q_0(i)$ plot as a function of temperature in figure 3 using an arbitrary reference temperature of 214.2 K. These values define the variation of the lattice parameters with temperature for the ice formed in the pores and are discussed further in section 5.

The overall intensities of all the Bragg peaks depend on temperature in a systematic manner and are higher at the lower temperatures. Figure 4 shows the variation for peaks 5, 7 and 8. This behaviour is associated with an increase in the crystalline component at the expense of the disordered water/ice phase between the crystal and the silica. A more detailed analysis of the overlapping triplet (peaks 1–3) is presented in the following paper (Seyed-Yazdi *et al* 2008).

Another way of demonstrating the phase changes is through the use of the temperature-difference function $\Delta D_{\text{M}}(Q, T; T_0)$ defined by equation (2). Figure 5 shows the variation in the diffraction pattern using a reference temperature, T_0, of 258 K, corresponding to the lowest temperature of the super-cooled water, prior to nucleation. The four plots show how the sharp crystalline peaks grow with a corresponding reduction in the broad peak at 1.8 Å^{-1} that arises from the disordered phase. The overall level at high-Q is near zero as required and confirms that there is little change in the amount of material in the beam; the small variation is probably due to changes in the inelasticity (Placzek) corrections arising from scattering by the deuterons. The low-Q (<1.5 Å^{-1}) region shows some variation in shape that is discussed in section 5.

4.3. Ice structure: peaks 1–3

The main ice peak in the region of 1.7 Å^{-1} has the expected asymmetric form with a shoulder on the low-Q side and a small peak on the broad wing of the high-Q side. The intensity profile for this peak is shown in figure 6 for a number of different temperatures on the cooling and warming runs. The data indicate that the general features of the profile do not change significantly and that the variation is both reversible and reproducible.

The shape of the composite triplet peak is attributed to the presence of stacking faults in the ice lattice (Kuhs *et al* 1987) and (Hansen 2007) as pure cubic ice will exhibit only a single peak at the centre of the triplet, at a Q-value of ∼1.7 Å^{-1}.

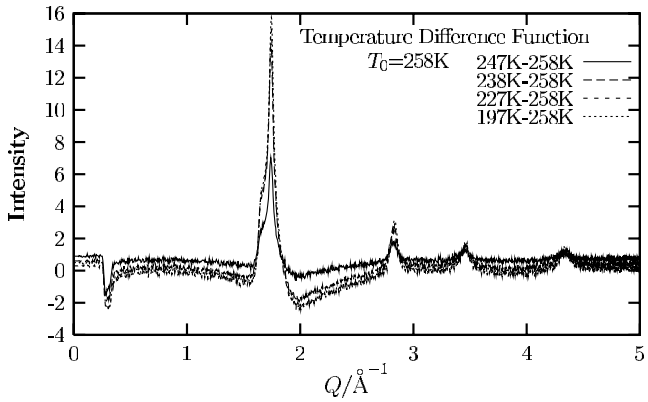

Figure 5. The temperature-difference function, $\Delta D_{\mathrm{M}}(Q, T; T_0)$, for the ice/water phases, with a reference temperature, T_0, of 258 K, showing the growth of $\mathrm{I_h}$ as the temperature is lowered.

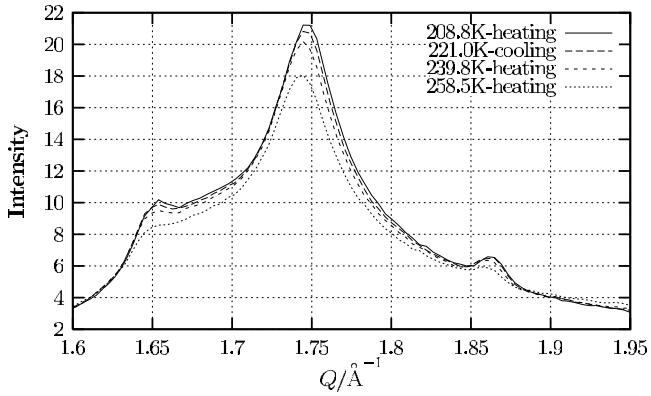

Figure 6. The peak profile, $I(Q)$, for various temperatures over the range 209–260 K.

It is also noticeable in figure 5 that there is a 'background' intensity between peaks 1–3 and peak 4 that is indicative of an underlying diffuse scattering component.

The profile of the composite peak, covering a Q-range of 1.5–1.9 Å^{-1}, changes very little with the changing temperature in each of the temperature cycles although there is a variation in its magnitude as shown in figure 6. There is also a minor component of hexagonal ice, as indicated by the small but well-defined peak at 1.86 Å^{-1}. If it is assumed that this component, with a relatively sharp 101 peak, is from a distinct region, then it is possible to use the $\mathrm{I_h}$ profile from the previous paper (Liu *et al* 2006). The width of this peak is comparable to the instrument resolution in this Q region (Hansen 2007). This subtraction has a small effect on the shape of the overall profile as shown in figure 7 for the rapid cooling run. The other changes lead to a modification of the shoulder on the low-Q side of the peak and a slight change in the overall peak amplitude. Corrections of this type bring the two separate runs into good agreement at all temperatures but suggest that the initial ice nucleation may be affected by the cooling rate as the quantity of hexagonal ice is seen to be different for the two scans. An alternative possibility is that the changes are brought about by the second cycle in the temperature sequence although it seems unlikely that there is any change

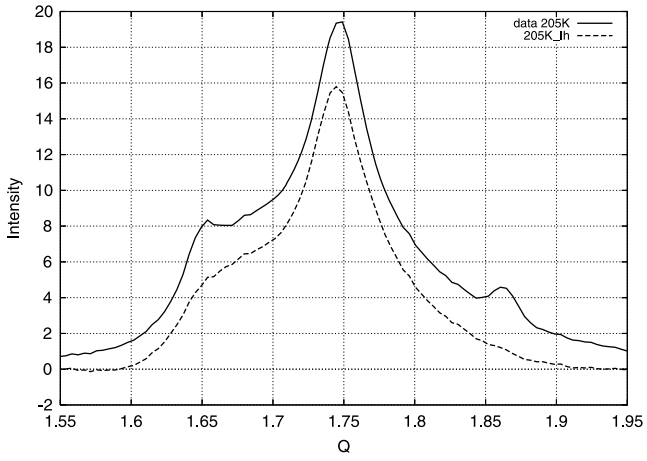

Figure 7. The profile of the main peak at 250 K before and after subtraction of a hexagonal ice component.

in the pore morphology for this case. Earlier studies of sol–gel silicas (Dunn *et al* 1988) showed that a sequence of freezing and thawing appeared to destroy the pore network for this material although measurements by NMR cryoporometry for other sol–gel silicas showed no change after several repeated freezing/thawing cycles.

It is clear that the resulting profile (figure 7) does not correspond to that of either hexagonal or cubic ice but retains features of both forms. The diffuse scattering contribution is also indicative of a disordered component but the exact nature of this contribution remains to be established (see section 5).

4.4. Normal and under-cooled water

It is known from earlier work on bulk water (Bellissent-Funel *et al* 1986) that the main peak in the diffraction pattern, Q_0, shifts systematically to lower Q-values as the temperature is reduced. This temperature variation, $Q_0(T)$, is indicative of enhanced hydrogen bonding at the lower temperatures and is interpreted as the build up of spatial correlations in the H-bonded network over an intermediate range, leading to an overall lower bulk density. The corresponding curve for confined water is displaced relative to that for bulk water but also indicates an extended range of hydrogen-bond correlations that is dependent on the pore size and varies with temperature in a similar manner. The change in the profile for the liquid phase in the present study is shown in figure 8. The peak displacement is clearly seen and there is also a variation in the low-Q region (figure 5) that is indicative of changes to the isothermal compressibility, although the extrapolation to $Q = 0$ cannot be made due to the strong SANS contribution from the pore structure, shown in figure 1(a).

A plot of the position in Q of the peak in the water profile in the SBA-15 pores is shown in figure 9. A comparative plot of the results for bulk water (Bosio *et al* 1981), the over-filled case for the present sample (Liu *et al* 2006) and the new results for the 'almost-filled' case are shown in figure 10, together with similar results from other mesoporous silicas. The general trend displays an increasing change as the temperature is reduced and follows the overall behaviour of the bulk water

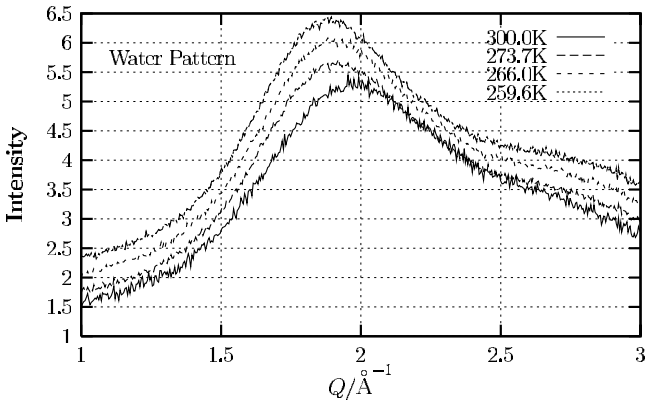

Figure 8. The variation with temperature for the water phase peak.

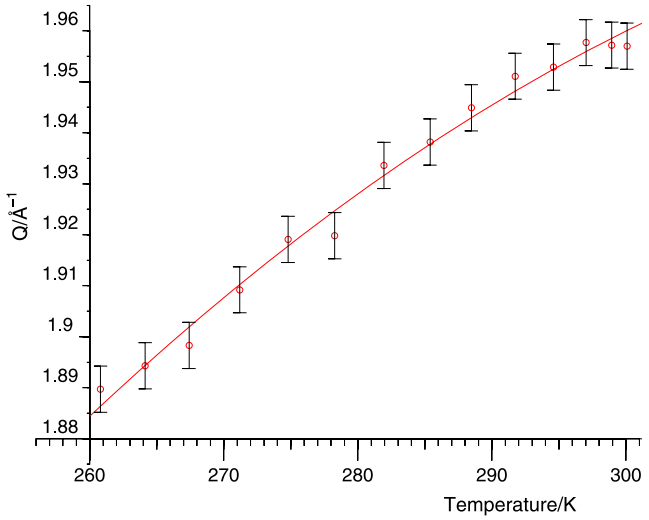

Figure 9. The temperature variation of the peak position, $Q_0(T)$, for the water phase, on a cooling ramp.

curve, except that the Q_0 values are lower. The displacement is correlated with pore size and has been interpreted in terms of enhanced spatial correlations in the smaller pores. The data with the largest displacement are early results for Gasil (Steytler *et al* 1983) with a nominal pore size of ∼25 Å and are not as reliable as the other datasets; they are included only to indicate the possible changes for water in a microporous silica network. The present measurements have a similar magnitude to the results for water in 150 Å sol–gel silicas, which indicates that the geometric effects could play a role in the changed freezing point depression and water structure. Further work on a wider range of micro and mesoporous silicas will be needed to fully answer this question.

The general change in the pattern is reflected more clearly in the temperature-difference function, $\Delta D_{\mathrm{M}}(Q, T; T_0)$, shown in figure 11 for a reference temperature, T_0, of 258 K, the lowest temperature for the 'fully-liquid' state on the cooling run. This pattern now seems to be universal for all studies to-date of under-cooled bulk water and is further established through the systematic behaviour of the isochoric temperature derivative (Dore *et al* 2000). The corresponding spatial

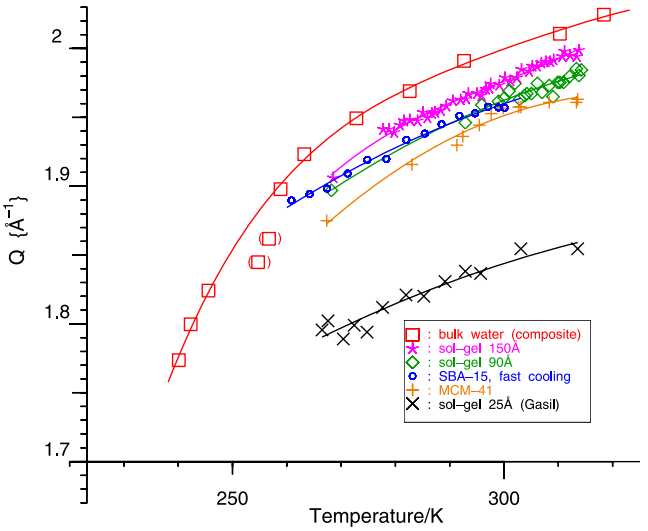

Figure 10. Comparative plots of $Q_0(T)$ for various studies of bulk and confined water.

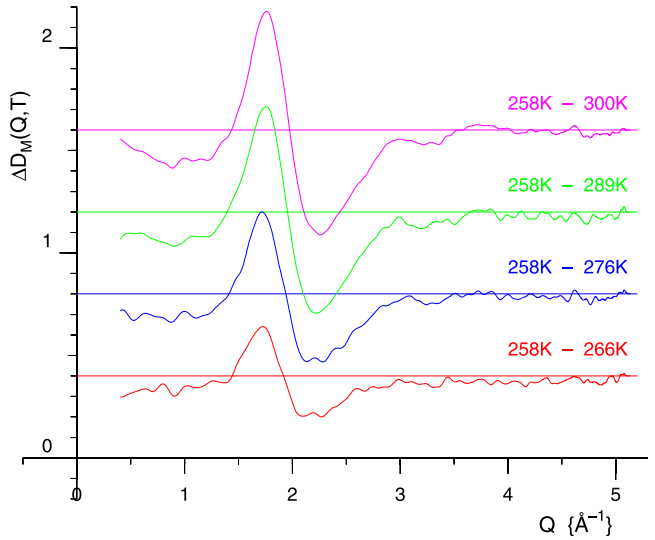

Figure 11. The temperature-difference function, $\Delta D_{\mathrm{M}}(Q, T; T_0)$, for the water phase, with a reference temperature, T_0, of 258 K.

function $\Delta d_l(r, T; T_0)/\Delta T$ appears unchanged for pairs of temperatures that have equivalent densities either side of the density maximum, except for the distance corresponding the hydrogen-bond. These results indicate that in the intermediate-range (5–15 Å), structural changes arising purely from thermal effects (i.e. irrespective of associated density variation for the equilibrium state at ambient pressure) are systematic and regular for water in its bulk liquid state. It is to be expected that a similar general behaviour will be seen in the confined water but the displacement of the peak is strongly dependent on the pore size and the simple behaviour may be influenced by specific water–substrate interactions. Furthermore, a similar check cannot be made in the present circumstances since the density of the confined water and its variation with temperature is not known.

The $\Delta D_{\mathrm{M}}(Q, T; T_0)$ function shown in figure 11 has a similar general pattern to all previous studies of bulk and confined water, including both sol–gel and MCM silicas. The peak shift shown in figure 9 results in a differential shape with a cross-over point for a Q-value of $\sim$1.95 Å^{-1}. There is also a subsidiary weak oscillation in the region of 3.0–3.8 Å^{-1} that is present in the data but partially obscured by the statistical spread of the data points. The magnitude of the function varies systematically with temperature, as expected. The universal nature of this curve indicates that the changes to the hydrogen-bonded network are similar for water in all conditions. The behaviour on an atomic scale suggests that the density falls with reduced temperature in a similar way to that for bulk water but there are no convenient ways of measuring the magnitude directly.

There is an interesting variation of the shape for the lower-Q region (0.4–1.2 Å^{-1}). The $\Delta D_{\mathrm{M}}(Q, T; T_0)$ function is normally plotted with respect to a chosen reference temperature, T_0, corresponding to the normal liquid state, with a value in the region of 295 K. The data in figure 11 use a low temperature reference of $T_0 = 258$ K that provides a different emphasis. The displacement in the general level of the $\Delta D_{\mathrm{M}}(Q, T; T_0)$ function in the region 0.5–1.0 Å implies a lower level for the compressibility as the temperature falls, but an accurate extrapolation to $Q = 0$ is not easy due to the SANS intensity and the variation of contrast arising from the change in density.

This type of behaviour is normal but the use of a lower temperature reference point reveals that the apparent change in the compressibility becomes less as the temperature is reduced. In contrast, the higher temperatures show a marked dip with a minimum in the region of 1 Å^{-1} that behaves systematically with temperature. However, there are significant changes in the slope between 276 and 300 K for Q-values below 1 Å^{-1}. The positive upturn becomes much larger in the higher temperature region. The data suggest the presence of a significant small-angle scattering intensity that is presumably centred on $Q = 0$ but is unfortunately outside the range of the observed measurements. A similar phenomenon has been observed in x-ray diffraction measurements on water/ice in MCM silicas (Dore *et al* 2002, figure 6) where the Q-range extended to lower values. The results showed a temperature-dependent intensity profile that became increasing large as the temperature was reduced to 182 K but was reversible as the temperature was increased. No specific comment was made in this paper as it was thought that the effect could have arisen from an artefact in the experimental arrangement used for the measurements. The re-appearance of a similar phenomenon in the neutron measurements indicates that a temperature-dependent small-angle scattering contribution could be present. Such a signal presumably arises, either from a changing contrast due to variations in the density of the water/ice or from intermediate-range density fluctuations in the liquid itself. In the latter case, the width of this component would be inversely proportional to the correlation length for the fluctuations. A plausible explanation of the variation shown in figure 11 is that the tail of a broad SANS distribution is seen in the higher temperature region and extends up to $\sim$1.0 Å^{-1}. As the temperature is reduced and the correlation length increases due to the formation of larger H-bonded 'clusters', the width becomes much smaller and the tail region is no longer within the accessible Q-range. This behaviour is therefore consistent with the normal assumptions relating to the overall response of the H-bonded network to temperature change, where the spatial correlations extend over longer length scales as the temperature is reduced. However, SANS and SAXS studies of bulk water (Bosio *et al* 1981, 1989, Xie *et al* 1993) do not exhibit a strong dependence on temperature so that the explanation remains unclear. Further studies in the low-Q region are obviously desirable to investigate this effect in a more systematic manner.

5. Interpretation

It is clear that the formation of ice in the 'almost-filled' SBA-sample is complex and involves a number of different processes. The two cooling/heating sequences indicate that there are some small differences in the ice formation in terms of the hexagonal component. It is unclear whether this effect is due to the fact that the initial freezing process results in changed conditions or whether it is dependent solely on the cooling rate; this characteristic is discussed in more detail in Paper 3 of the series. In earlier studies of sol–gel silicas (Dunn *et al* 1988) it was found that sequential freezing resulted in major changes to the subsequent ice nucleation that could be attributed to the damaging of the pore network, arising from mechanical stress caused by expansion during the ice formation. This effect is much less likely in the case of the templated silicas as the wall thickness is larger and the relative pore volume is less. Alternatively, the process of freezing could have led to a re-distribution of the water/ice in the available pore volume. This feature would occur if the volume expansion due to the transformation of water into ice actually caused the expulsion of some of the pore water onto the external surfaces. However any external ice would not be expected to melt at the lower temperature in the warming cycle so that the observed reversibility seems to rule out this possibility. The quantitative analysis of the ice growth has been conducted on the assumption that this small quantity of hexagonal ice is incorporated into the pores as a natural consequence of the ice nucleation process and does not arise from any ice formation outside the pore network. Nevertheless, it would be interesting to investigate the ice formed in a very rapid cooling process, such as the 'flash-cooling' methods used in biological studies (Weik *et al* 2005a) or the rapid nucleation of metastable water from a 'stretched' state (Williams and Williams 2004)

The low-angle neutron diffraction studies of a fast-frozen sample of bacterio-rhodopsin by Weik are relevant to this question. The measurements give a direct indication of the membrane layer spacing in the sample, which exhibits a significant change in the region of 200–220 K. The movement of the peaks indicates that the layer spacing increases and therefore that there must be some mobility in the 'ice' volume. Consequently, there appears to be a pre-melting phenomenon when the sample is heated to temperatures above 200 K such that re-ordering and translational displacement occurs over

a mesoscopic range. The measurements do not include the diffraction peaks for the ice and therefore the form of ice is not defined. A similar behaviour has now been observed in other samples of biological interest (Weik *et al* 2005b). It seems likely that it represents another manifestation of the formation of a mobile form of ice arising from the 'softening' of the brittle ice network formed in this case by a rapid quench to much lower temperatures. Whether this behaviour is a manifestation of the existence of the conjectured 'high density' water (Mishima and Stanley 1998) is a matter for further debate.

The characteristics of the liquid state in the SBA-sample seem to follow the expected behaviour, indicating an increase in the hydrogen bonding as the temperature is reduced. The temperature-difference function exhibits the usual features seen previously for both bulk and confined water (Webber and Dore 2004) However, the data display an interesting variation in the low-Q region (0.4–0.6 Å^{-1}) that requires further investigation using a different instrument to probe lower Q-values. The observed variation of the 'tail' region implies a correlation length of ∼100 Å or more, so that the magnitude of the correlation length is comparable with the dimensions of the pore. It seems feasible that this value could be related to the size of transient proto-crystallites and would therefore be of direct significance to the process of nucleation. It is intended to undertake a further study of this effect in a later experiment.

6. Conclusions

The present results indicate a complex relationship for the phases of water/ice in the confined geometry of the SBA-15 sample. The general behaviour is similar to that observed in previous work but has enabled a greater degree of detail to be observed and led to some variations in the interpretation. The overall conclusions for a case where the internal volume is almost completely occupied by water can be summarized as:-

- the formation of ice in the pores occurs at a temperature that is below that for bulk materials and is well-defined,
- the displacement of the main diffraction peak for the water phase shows the same form, $Q_0(T)$, of earlier studies, indicating enhanced hydrogen bonding and network correlations for the confined phase as the temperature is reduced,
- the primary nucleation event leads to the formation of a defective form of ice-I, which has predominantly cubic ice features and a small admixture of hexagonal ice component that appears to depend on either the cooling rate or the thermal history,
- the magnitude of the cubic ice component shows systematic variation over a wide temperature range and the broad triplet peak profile retains the same shape at all temperatures,
- there is diffuse scattering between the Bragg peaks that indicates some disorder in the confined material and is discussed more fully in the following paper (Seyed-Yazdi *et al* 2008).
- the low-Q region (0.6–1.0 Å^{-1}) for the liquid phase shows evidence of a SANS component that may relate to density fluctuations with an intermediate correlation length that becomes large, just prior to nucleation.

Paper 1 (Liu *et al* 2006) in this series has discussed the temperature variation of the ice component as a function of temperature. It is conjectured that there is an interfacial region between the central ice crystallite and the silica surface that contains a disordered form of water/ice. As the temperature is reduced this interfacial layer is incorporated into the ice crystallite but subsequently returns to its initial form as the temperature is raised. This behaviour suggests an equilibrium between the phases that determines and defines the reversible features that are observed. The nature of this disordered layer is difficult to characterize but clearly allows rotational movement of the water molecules at low temperatures. NMR studies (Webber *et al* 2007a, 2007b) suggest that the behaviour is intermediate between that of bulk phases of water and ice. This layered material has been termed 'plastic ice' in analogy with the plastic crystal phase, where the regular lattice structure is partially disordered by either static or dynamic rotational correlations. The studies of Weik (Weik *et al* 2005a) provide a separate indication of the mesoscopic mobility of this state and its onset in the region of 200 K.

The current paper represents the second in a series of publications centred on the neutron study of the states of ice/water in confined geometry. Further analysis of the triplet peak profile by a peak-fitting routine is addressed in Paper 3. The analysis of partially-filled samples with filling factors of 0.6 and 0.4 using the same SBA-15 material will be published later as Paper 4. Additionally, a corresponding study for water/ice in a different SBA-15 sample with a pore diameter of 62 Å has been made under the same experimental conditions. These additional measurements provide information that is specifically linked to pore-size effects involving cylindrical pores with a hydrophilic interface. A diffraction experiment for investigating the characteristics of water and ice in a surface-modified, 'mainly hydrophobic' silica (Castricum *et al* 2006) has also been made and will be reported separately (Jalassi *et al* 2008).

Acknowledgments

The experimental work was carried out within the general neutron programme of the EPSRC, supporting the use of European facilities such as the ILL. One of us (JBWW) was partially supported by collaborations with the BMFFFS Project (Behaviour and Modelling of Faults/Fractures/Fluids Systems) and the Centre for Gas Hydrate Research, both in the Institute of Petroleum Engineering, Heriot-Watt University, and is currently partially supported in conjunction with the Centre for Gas Hydrate Research by EPSRC grant EP/D052556/1. The work in Berlin, involving the fabrication and characterization of the SBA-material, was supported by the Deutsche Forschungsgemeinschaft in the framework of the SFB 448 'Mesoscopically Organized Composites'. One of us (JS-Y) wishes to thank the Iranian Ministry of Science and

Technology and the British Council for a grant to enable her to work with the neutron group at UKC.

Appendix

Neutron diffraction measurements have been made for this sample using a shorter wavelength in order to cover a wider Q-range. The results for the silica plus water, the dry silica and the empty cryostat are shown in figure A.1 for a temperature of 200 K. An inset, showing the region of 1.0–2.3 $Å^{-1}$ after subtraction of the dry silica, indicates the loss of Q-resolution for this case in comparison with the results for the D20 instrument. The runs were made at a fixed temperature as a much longer counting time is required to build up adequate statistics. After correction for Placzek effects to the self-term, the data may be converted to a real-space pair distribution function by use of the Fourier transform and gives the $d(r)$ data shown in figure A.2(a). The first two sharp peaks correspond to the intra-molecular OD and DD peaks and the additional peaks correspond primarily to correlations within the cubic ice structure as the correlations for the amorphous ice are much reduced in size. This feature can easily be seen in the difference function for the transition from lda-ice to cubic ice at 140 K (Blakey 1994) that is shown in figure A.2(b) and was measured in an earlier experiment on a similar liquids diffractometer with an identical Q-range. In this case the local correlations due to the intra-molecular terms and the local H bonding are removed and the figure displays the spatial features of the cubic ice. The overall behaviour of the two curves above 6 Å is immediately apparent and the additional oscillatory structure in the 3–6 Å region for figure A.2(b) is primarily due to residual effects from the original lda-ice structure.

These curves show that measurements over a wide Q-range using a conventional liquids diffractometer are incapable of providing the discrimination that has been obtained with the use of the D20 instrument. Although a smaller Q-range is covered, the improved Q-resolution enables the different components of the crystalline and disordered structures to be identified in a quantitative manner that is impossible from the Fourier transform approach.

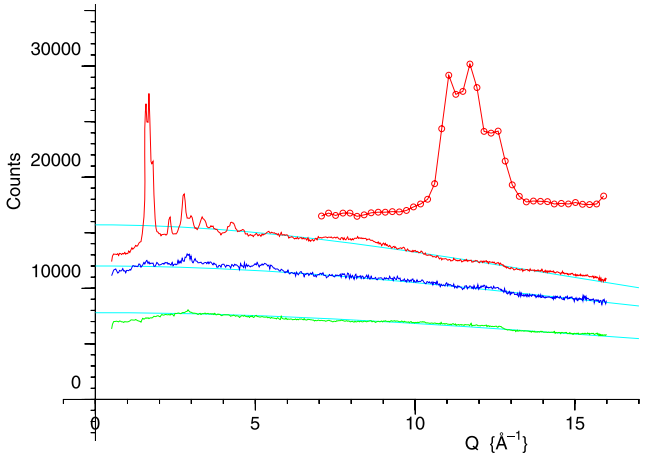

Figure A.1. Wide Q-range diffraction data for D_2O in SBA-15, at a temperature of 200 K.

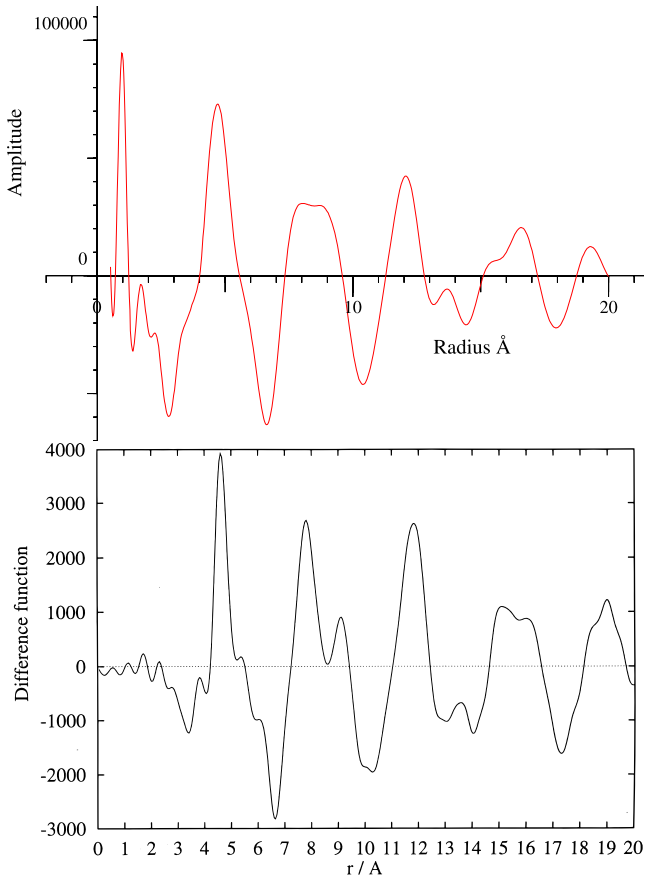

Figure A.2. (a) $d(r)$ for D_2O in SBA-15, at a temperature of 200 K. (b) $d(r)$ difference function for the transition from lda-ice to cubic ice at 140 K.

References

Bellissent-Funel M C, Teixeira J, Bosio L, Dore J and Chieux P 1986 *Europhys. Lett.* **2** 241–5

Blakey D M 1994 Structural studies of vapour-deposited amorphous-ice and argon/amorphous-ice systems by neutron diffraction *PhD Thesis* Physics, University of Kent at Canterbury, UK

Bosio L, Teixeira J and Bellissent-Funel M C 1989 *Phys. Rev.* A **39** 6612–3

Bosio L, Teixeira J and Stanley H E 1981 *Phys. Rev. Lett.* **46** 597–600

Castricum H L, Mittelmeijer-Hazeleger M C, Sah A and ten Elshof J E 2006 *Micropor. Mesopor. Mater.* **88** 63–71

Dore J C, Sufi M A M and Bellissent-Funel M C 2000 *Phys. Chem. Chem. Phys.* **2** 1599–602

Dore J C, Webber B, Behrens P, Haggenmuller C and Montague D 2002 New kinds of phase transitions: transformation in disordered substances *Nato Science Series, Series II: Mathematics, Physics and Chemistry* 81st edn, ed V V Brazhkin, S V Buldrev, V N Ryzhov and H E Stanley (Netherlands: Kluwer–Academic) pp 469–80

Dunn M, Dore J C and Chieux P 1988 *J. Cryst. Growth* **92** 233–8

Evans W A B 1997 *Advanced Numerical Techniques* Physics Laboratory, University of Kent, PH611

Grünberg B, Emmler T, Gedat E, Shenderovich I, Findenegg G H, Limbach H-H and Buntkowsky G 2004 *Chem. Eur. J.* **10** 5689–96

Hansen T C 2007 private communication

Hansen T C, Henry P F, Fischer H E, Torregrossa J and Convert P 2008 *Meas. Sci. Technol.* **19** 034001 http://stacks.iop.org/0957-0233/19/034001

Jalassi J, Dore J C, Webber J B W and Bellissent-Funel M C 2008 in preparation
Kuhs W F, Bliss D V and Finney J L 1987 *J. Physique* **48** 631–6
Liu E, Dore J C, Webber J B W, Khushalani D, Jähnert S, Findenegg G H and Hansen T 2006 *J. Phys.: Condens. Matter* **18** 10009–28 http://stacks.iop.org/0953-8984/18/10009
Mishima O and Stanley H E 1998 *Nature* **396** 329–35
Schreiber A, Ketelsen I and Findenegg G H 2001 *Phys. Chem. Chem. Phys.* **3** 1185–95
Seyed-Yazdi J, Farman H, Dore J C, Webber J B W and Findenegg G H 2008 *J. Phys.: Condens. Matter* **20** 205108
Steytler D C, Dore J C and Wright C J 1983 *Mol. Phys.* **48** 1031–51
Webber J B W, Anderson R, Strange John H and Tohidi B 2007a *Magn. Reson. Imaging* **25** 533–6 http://dx.doi.org/doi:10.1016/j.mri.2006.11.022
Webber J B W and Dore J C 2004 *J. Phys.: Condens. Matter* **16** S5449–70 (Special Issue: Water in Confined Geometry) http://stacks.iop.org/JPhysCM/16/S5449
Webber J B W and Dore J C 2008 *Nucl. Instrum. Methods* A **586** 356–66 http://dx.doi.org/10.1016/j.nima.2007.12.004
Webber J B W, Dore J C, Strange John H, Anderson R and Tohidi B 2007b *J. Phys.: Condens. Matter* **19** 415117
Weik M, Lehnert U and Zaccai G 2005a *Biophys. J.* **89** 3639–46
Weik M, Schreurs A M M, Leiros H K S, Zaccai G, Ravelli R B G and Gros P 2005b *J. Synchrotron Radiat.* **12** 310–7
Williams P R and Williams R L 2004 *Mol. Phys.* **102** 2091–102 http://dx.doi.org/10.1080/00268970412331292786
Xie Y L, Ludwig K F, Morales G, Hare D E and Sorensen C M 1993 *Phys. Rev. Lett.* **71** 2050–3